J Mater Sci (2007) 42:9440–9446
DOI 10.1007/s10853-007-1843-z

Interfacial energy determination of nano-scale precipitates by CALPHAD description of Gibbs–Thomson effect

Sina Shahandeh · Hamed Arami · S. K. Sadrnezhaad

Received: 11 November 2006 / Accepted: 9 May 2007 / Published online: 27 July 2007

Abstract A theory based on calculation of phase diagrams in the binary systems was developed that describes Gibbs–Thomson effect. In this model effect of both interfacial energy and interface confinement (Laplace–Young pressure) are included in energy shift of alloys and phases. By using the CALPHAD model, interfacial energy of Cu_4Ti precipitates in Cu–Ti system was obtained which shows better consistency with experimental results of Gibbs–Thomson effect of 10–20 nm radius precipitates.

Introduction

Usually experimental values of interfacial energy of precipitates are scattered in a wide range. Most of the mentioned data are obtained from coarsening experiments. Size evolution of the particles can be measured by TEM, SAXS or SANS and by relating their size distribution to aging time and use of Lifshitz–Slyozov–Wagner (LSW) theory [1, 2], or its modified versions [3], the interphase interfacial energy can be calculated as follows:

$$r^3 - r_0^3 = Kt \tag{1a}$$

$$K = \frac{8D\sigma_{\alpha\beta}V_m^{\beta}C_B^{\alpha}\left(1 - C_B^{\alpha}\right)}{9RT\left(C_B^{\beta} - C_B^{\alpha}\right)^2} \tag{1b}$$

where r is the mean radius of precipitates in time t and r_0 is initial radius of the particles. $\sigma_{\alpha\beta}$ is the interfacial energy, C_B^{α} and C_B^{β} are equilibrium concentration of B in α (matrix) and β (precipitate) phases, respectively, D is the interdiffusion coefficient of B in the matrix and V_m^{β} is molar volume of precipitate phase. As it is seen, the diffusivity of the atoms in the system is also necessary for determination of $\sigma_{\alpha\ \beta}$, which itself has noticeable scattered values. Therefore, besides the unavoidable experimental errors in estimation of size distribution of the precipitates, this will also result in uncertain values for interfacial energy.

On the other hand, the governing driving force for coarsening is the difference between matrix concentration in the vicinity of small and large particles, which leads to diffusion flux of solute atoms from smaller particles to larger ones. This phenomenon is caused by Gibbs–Thomson effect that changes the phase equilibria between nano-sized precipitates and matrix and also increases the solute concentration around small particles due to interfacial curvature.

Different models were proposed for describing this effect. First model was proposed by Thomson [4], Gibbs [5] and Freundlich [6], which is known as Gibbs–Thomson formula:

$$X_B^{\alpha}(r) = X_B^{\alpha}(\infty)\exp\left(\frac{2\sigma_{\alpha\beta}V_m^{\beta}}{RTr}\right) \tag{2}$$

This model directly relates the equilibrium matrix concentration to the radius of particles. By use of analytical electron microscopy [7] or electrical resistivity measurements [8], one can evaluate matrix concentration around the precipitates and calculate the interfacial energy of the particles, considering Gibbs–Thomson effect. The remaining part is finding an accurate model for this effect.

S. Shahandeh · H. Arami · S. K. Sadrnezhaad (✉)
Materials and Energy Research Center, P.O. Box 14155-4777, Tehran, Iran
e-mail: sadrnezh@sharif.edu

In this study we proposed a theoretical model based on CALPHAD method for describing Gibbs–Thomson effect in binary alloys and compared it with other formulas. Then this method was used to find coherent interfacial energy of Cu_4Ti in FCC Cu–Ti matrix.

Gibbs–Thomson effect in binary alloys

In this section some formulas for dilute and concentrated binary alloys are summarized. The simplest relation is Eq. 2 that assumes some simplifications that are not real for most of the alloy systems, such as dilute solution behavior of the matrix phase and $X_B = 1$ for precipitates. In Hillert [9] formula for dilute alloys the concentration of precipitate is included:

$$\left(1 - X_B^{\beta}\right) \ln\left(\frac{1 - X_B^{\alpha}(r)}{1 - X_B^{\alpha}(\infty)}\right) + X_B^{\beta} \ln\left(\frac{X_B^{\alpha}(r)}{X_B^{\alpha}(\infty)}\right) = \frac{2\sigma_{\alpha\beta} V_m^{\beta}}{RTr} \tag{3}$$

Better models should embrace more complicated thermodynamics for matrix solution. Therefore, concentrated solution behavior of matrix is included in Darken factor [10]:

$$X_B^{\alpha}(r) = X_B^{\alpha}(\infty)\left(1 + \frac{1 - X_B^{\alpha}(\infty)}{X_B^{\beta}(\infty) - X_B^{\alpha}(\infty)} \frac{2\sigma_{\alpha\beta} V_m^{\beta}}{RTre_B^{\alpha}(X_B^{\alpha}(\infty))}\right) \tag{4}$$

where e_B^{α} is function of X_B^{α} and is given by:

$$e_B^{\alpha}\left(X_B^{\alpha}\right) = 1 + \left(\frac{\partial \ln \gamma_B^{\alpha}}{\partial \ln X_B^{\alpha}}\right) \tag{5}$$

where γ_B^{α} is activity coefficient of B in matrix. This model has a simplification of the small variation of matrix composition at curved interfaces. The formula of Qian and Lim [11] uses Darken factor and dose not have this simplification:

$$\left(1 - X_B^{\beta}\right) \ln\left(\frac{1 - X_B^{\alpha}(r)}{1 - X_B^{\alpha}(\infty)}\right) + X_B^{\beta} \ln\left(\frac{X_B^{\alpha}(r)}{X_B^{\alpha}(\infty)}\right) = \frac{2\sigma_{\alpha\beta} V_m^{\beta}}{RTre_B^{\alpha}(X_B^{\alpha}(\infty))} \tag{6}$$

Note that Darken factor is only evaluated at $X_B^{\alpha}(\infty)$, the equilibrium concentration of matrix at flat interface. More accurate result can be obtained if one considers thermodynamic behavior of matrix phase at higher concentrations at curved interface. This was included in a formula by Martin and Doherty [12]:

$$\ln\left(\frac{X_B^{\alpha}(r)}{X_B^{\alpha}(\infty)}\right) = \left(\frac{1 - X_B^{\alpha}(r)}{X_B^{\beta}(\infty) - X_B^{\alpha}(\infty)} \frac{2\sigma_{\alpha\beta} V_m^{\beta}}{RTr}\right) - \ln\left(\frac{\gamma_{\alpha}\left(X_B^{\alpha}(r)\right)}{\gamma_{\alpha}(X_B^{\alpha}(\infty))}\right) \tag{7}$$

where $\gamma_{\alpha}\left(X_B^{\alpha}(r)\right)$ is activity coefficient of B in matrix near small precipitate. Equations 3, 6 and 7 are implicit and should be solved versus $X_B^{\alpha}(r)$ to find matrix concentration in equilibrium with a particle with radius r.

All of these models were developed based on assumption of constant precipitate concentration [11, 13]. Comparison between these formulas and some of their simplifications can also be found in references [11, 13, 14]. Readers are referred to the reference of each model for their proof and derivation.

CALPHAD model for Gibbs–Thomson effect in binary alloys

The decrease in curvature of precipitates with sizes smaller than 100 nm results in appearance of two effects; first is an increase of the total interfacial area per constant volume of precipitates [15] and second is an increase of internal pressure that is called Laplace–Young pressure [16]. In most of the previous articles, the internal pressure was introduced as the only governing reason for Gibbs free energy shift of the precipitates and consequently occurrence of Gibbs–Thomson effect. As it will be shown, although this leads to correct answers, from thermodynamics points of view, another term should also be included to obtain more accurate results.

Gibbs free energy of precipitate and matrix will be changed with the formation of nano-structures; the simplest case is small spherical precipitates in infinite matrix. If we assume that a microstructure consists of n_p particles with mean radius of r_p, the total interphase interface is $S_p = 4\pi r^2 n_p$. For one mole of precipitate the total volume is V_m^{β}, therefore one mole of β consists of $n_p = V_m^{\beta}/\frac{4}{3}\pi r^3$ particles. Thus, by substitution, the additional energy of interface (ΔG_s) is:

$$\Delta G_s = S_p \cdot \sigma_{\text{interface}} = \frac{3\sigma_{\text{interface}} V_m^{\beta}}{r} \tag{8}$$

In addition, when the interface confines a small particle, the surface tension around the precipitate causes an internal pressure inside the particle. This pressure which is radius dependent is [17]:

$$\Delta P = \frac{2\sigma_{\text{interface}}}{r} \tag{9}$$

This pressure causes an increase in Gibbs free energy of the phase, which can be expressed in form of $dG = VdP - SdT$. Because temperature is constant and molar volume of precipitates is assumed to be constant with variation of P, the Gibbs energy shift due to Laplace–Young pressure (Eq. 9), can be written in the form of:

$$\Delta G = \frac{2\sigma_{\text{interface}}}{r} V_m \tag{10}$$

Contribution of these two parameters changes the Gibbs free energy of matrix and precipitate and consequently the state of equilibrium between them. Figure 1 shows a thermodynamic loop between two states of bulk phases and nano-size precipitates. In state 1 both phases with free energy of $G^{\alpha}(\infty)$ and $G^{\beta}(\infty)$, and composition of $X_B^{\alpha}(\infty)$ and $X_B^{\beta}(\infty)$, are in equilibrium. In state 3 disperse spherical precipitates are inside matrix phase. One of the aims of this study is to determine the difference between energy of each phase in the states 1 and 3. Because Gibbs energy is independent of path, we can define an auxiliary state between them and move toward state 1 to 2 and then to 3. In state 2, β phase is divided into the same volume of spherical precipitate with radius r. Also inside α phase, there is the same number of spherical holes with the same radius. In this state the additional surface energy for β is $\Delta G_s^{\beta} = 3\sigma_{\beta} V_m^{\beta}/r$ and for α is $\Delta G_s^{\alpha} = 3V_m^{\beta}/r \times \sigma_{\alpha}$, where σ_{α} and σ_{β} are interfacial energy of phases in equilibrium with their vapors. β phase also has the additional energy of Laplace–Young pressure which is $\Delta G_P^{\beta} = 2\sigma_{\beta} V_m^{\beta}/r$. When we put into α holes the free surface of particles and matrix is replaced with interphase interface. In the same way one can simply find the energy variations as it is shown in Fig. 1. By adding energy change of path 1-2-3, energy change between states 1 and 3 can be found:

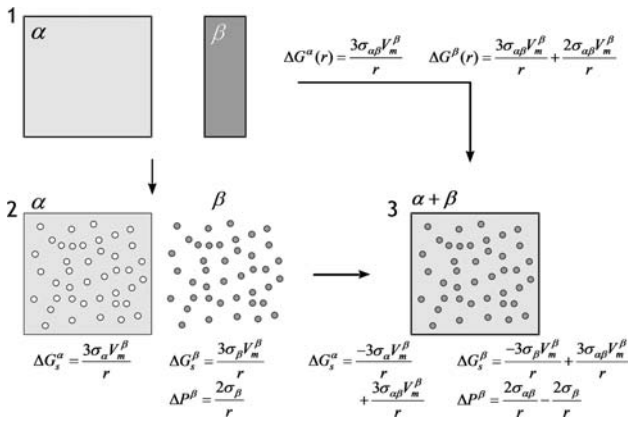

Fig. 1 Variation of the Gibbs free energy of matrix and precipitate between two conditions of bulk phase and nano-scale precipitates. Total energy change from path 1 to 3 is equal to state 1 to intermediate state 2 and then to final state 3

$$\Delta G_r^{\alpha}(r) = \frac{3\sigma_{\alpha\beta} V_m^{\beta}}{r} \tag{11a}$$

$$\Delta G_r^{\beta}(r) = \frac{3\sigma_{\alpha\beta} V_m^{\beta}}{r} + \frac{2\sigma_{\alpha\beta} V_m^{\beta}}{r} \tag{11b}$$

These additional energies are not equal and therefore, they will alter the state of equilibrium. For finding equilibrium point one should use CALPHAD methods.

Two methods can be used for finding the equilibrium in binary systems. One is tangent construction [18] and solution of two nonlinear equations and the other is minimization of total energy that is more common in CALPHAD techniques [19]. For describing the Gibbs–Thomson effect in binary alloys one should add the excess energy of the interface and Laplace–Young (Eq. 11) to the Gibbs free energy of mixing and minimize the total energy. A starting point and an alloy point are necessary for running of the optimization algorithm. Figure 2 shows mixing energy of matrix and precipitate phases. Decreasing the size of the precipitates shifts the curves to higher levels of energy, which alters the minimum point in Gibbs energy-composition space. The assumed alloy point is in the middle of two starting points in the free energy curves of α and β phases (Fig. 2, cross marker). The total energy of this alloy can be expressed as:

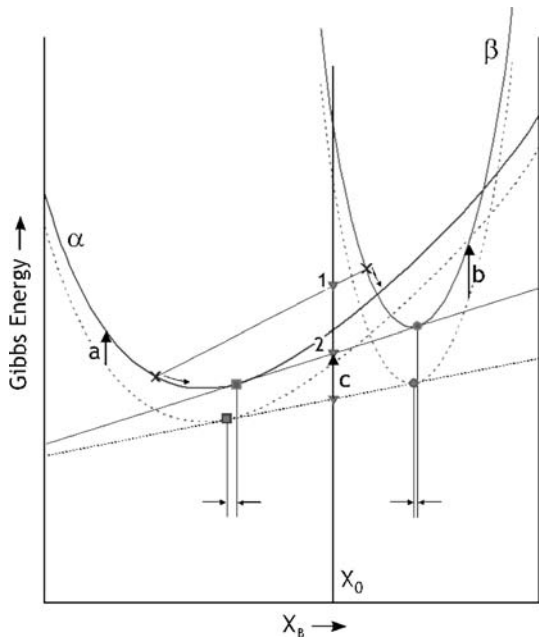

Fig. 2 Gibbs free energy of matrix and precipitate phases. Dashed line is for bulk phase and solid line is for nanometer scale precipitates. Cross points are initial equilibrium compositions which move to real equilibria points by optimization of the total energy. Total energy decreases from point 1 to 2 by optimization process. The consequence of the energy shift is the change of equilibrium composition of the matrix and precipitate which is indicated by pointed arrows

$$G^{X_0}(X_B^{\alpha}, X_B^{\beta}) = f^{\alpha}\Delta G^{\alpha}_{\mathrm{mix},r}(X_B^{\alpha}) + f^{\beta}\Delta G^{\beta}_{\mathrm{mix},r}(X_B^{\beta}) \quad (12)$$

where $\Delta G^{\alpha,\beta}_{\mathrm{mix},r}$ is mixing Gibbs free energy of α and β plus additional energy of interface $(\Delta G_r^{\alpha,\beta})$. $f^{\alpha,\beta}$ is molar fraction of the phases, which can be found by lever rule. As it is shown in Fig. 2, by moving through equilibrium composition in Gibbs energy curves, total energy of the alloy decreases from point 1 to 2. This process is governed by optimization algorithm which minimizes two variable function $G^{X_0}(X_B^{\alpha}, X_B^{\beta})$.

All of the previous models (Eqs. 2–6) assume that X_B^{β} is constant, but as it can be seen, the precipitate composition should also vary with energy shift. The amount of mutual composition change is depending on the shape of Gibbs free energy curves of the matrix and precipitate. Therefore, in some cases this assumption can lead to considerable inaccuracy. On the other hand, CALPHAD model has no assumption for thermodynamic behavior of solution or for composition change.

Another important point that was forgotten in previous models is energy shift of the matrix. Consider a particular alloy with composition X_0, that transforms into matrix and precipitate phases with compositions X_B^{α} (∞) and X_B^{β} (∞) and molar fractions of f^{α} and f^{β}, respectively. When β disperses into small particles there is a shift in energy of alloy with respect to the bulk condition. This energy shift of the alloy is shown with arrow "c" in Fig. 2. This shift has two components, one for additional energy of the precipitate (arrow b) and the other for additional energy of the matrix (arrow a). If like previous models, only the Laplace–Young pressure is considered for calculation of the energy shift of the phases, the contribution of the additional interphase interface to the additional energy of the alloy will be neglected. In this model, additional interfacial energy is also added to the total free energy of α and β phases, which leads to calculation of the actual Gibbs free energy of the alloy. This is important especially if another phase with dimensions different from the particles is in equilibrium with matrix or precipitate. In this case, variation of the Gibbs energy changes the equilibrium composition. However, in two-phase systems, the interfacial energy does not change the equilibria significantly, since both matrix and precipitate gain the same additional energy.

Details of CALPHAD method will be discussed in finding interfacial energy of Cu_4Ti in Cu–Ti system.

Interfacial energy of Cu_4Ti precipitates

Generally, in the Gibbs–Thomson effect and other interface related phenomena interface characteristics are unknown. Although it is possible to measure the increase of solute concentration around the particles, no one really knows the reasons such as interface tension and energy.

The measured values for interfacial energy of Cu_4Ti phase are scattered. The values of 67 mJ/m^2 [20] and 31 mJ/m^2 [21] were measured. Also, Bourchers et al. [22] calculated value of 47 mJ/m^2 by pair interaction model. Another accurate experimental result was obtained by Miyazaki et al. [23]. They measured concentration of the matrix in equilibrium with the precipitates by macroscopic composition gradient method. Particles radius varied from 9 nm to 27 nm. They also calculated the interfacial energy of Cu_4Ti precipitates by linear version of Gibbs–Thomson formula (Eq. 2). Because of low accuracy of that formula they reported the value of 100 mJ/m^2. Equation 2 underestimates composition changes; therefore it results in higher interfacial energy to compensate its low variation rate. Qian and Lim [24] used a formula similar to Eq. 3 to re-evaluate experimental results of Miyazaki et al. In their work, a better model for dilute binary systems led to values of 53 mJ/m^2 (at 823 K) and 63 mJ/m^2 (at 873 K) that are the most reasonable results obtained for the interfacial energy of Cu_4Ti precipitates. In this model some simplifications were incorporated such as dilute solution behavior for matrix and precipitate phases and constant precipitate composition.

In order to minimize Eq. 12 as a function of matrix and precipitate compositions, one should know values of $\Delta G^{\alpha}_{\mathrm{mix}}$ and $\Delta G^{\beta}_{\mathrm{mix}}$. Advantage of CALPHAD method is that it uses a versatile solution thermodynamics model. In this system thermodynamic behavior of FCC matrix phase was described by a semi-regular model and for complex intermetallic precipitates sublattice model [19] was used. Assuming a single lattice random solid solution for matrix, the mixing free energy of the matrix can be written in form of:

$$\Delta G^{\alpha}_{\mathrm{mix}} = \sum_i X_i^{\alpha}\,{}^0G_i + RT\sum_i X_i^{\alpha}\ln(X_i^{\alpha}) + \sum_i^{n-1}\sum_{j=i+1}^{n} X_i^{\alpha}X_j^{\alpha}\Omega_{i,j} \quad (13)$$

where ${}^0G_i$ is the difference between Gibbs energy of element i in reference state and in FCC phase. $\Omega_{i,j}$ is binary interaction parameter and based on Ridlich–Kister formalism [19] it can be expanded as:

$$\begin{aligned}\Omega_{i,j} &= \sum_k \Omega_{i,j}^k (X_i - X_j)^k \\ \Omega_{i,j}^k &= a_k + b_k T\end{aligned} \quad (14)$$

Kumar et al. [25] modeled Cu_4Ti precipitates which consisted of two sublattices one for Cu and one for Ti. The anti-structural atoms in the sublattices form wide homogeneity range of this phase. Using sublattice formalism for $(Cu, Ti)_4(Cu, Ti)$, the free energy of Cu_4Ti can be formulated:

$$\begin{aligned}\Delta G_{\text{mix}}^{\text{Cu}_4\text{Ti}} &= y_{\text{Cu}}^1 y_{\text{Ti}}^2 {}^0G_{\text{Cu:Cu}} + y_{\text{Cu}}^1 y_{\text{Ti}}^2 {}^0G_{\text{Cu:Ti}} \\ &+ y_{\text{Ti}}^1 y_{\text{Cu}}^2 {}^0G_{\text{Ti:Cu}} + y_{\text{Ti}}^1 y_{\text{Ti}}^2 {}^0G_{\text{Ti:Ti}} \\ &+ RT\left[4\sum_i y_i^1 \ln y_i^1 + \sum_i y_i^2 \ln y_i^2\right] \\ &+ y_{\text{Cu}}^1 y_{\text{Ti}}^1 (y_{\text{Cu}}^2 L_{\text{Cu,Ti:Cu}} + y_{\text{Ti}}^2 L_{\text{Cu,Ti:Ti}}) \\ &+ y_{\text{Cu}}^2 y_{\text{Ti}}^2 (y_{\text{Cu}}^1 L_{\text{Cu,Cu:Ti}} + y_{\text{Ti}}^2 L_{\text{Cu,Ti:Ti}}) \end{aligned} \quad (15)$$

where y_i^s is fractional site occupation and is defined as the ratio of number of i atoms in sublattice s to the total number of sites in the sublattice. Therefore, the molar fraction of i atoms can be expressed as $X_i = 0.8y_i^1 + 0.2y_i^2$. In this model four first terms stand for Gibbs energy reference state with these constrains:

$$\begin{aligned} {}^0G_{\text{Cu:Cu}} &= 25,000\,\text{J/mol}, \quad {}^0G_{\text{Ti:Ti}} = 25,000\,\text{J/mol} \\ {}^0G_{\text{Ti:Cu}} &= {}^0G_{\text{Cu:Cu}} + {}^0G_{\text{Ti:Ti}} - {}^0G_{\text{Cu:Ti}} \end{aligned} \quad (16)$$

The parameters indicated as ${}^0G_{A:B}$ correspond to the Gibbs energy of the stoichiometric compound $A_a\,B_b$ that is related to the formation energies and elements standard reference states:

$${}^0\Delta G_{A:B}^{A_aB_b} = \Delta H_f^{A_aB_b} - T\Delta S_f^{A_aB_b} + a\,{}^0G_A^{\text{ref}} + b\,{}^0G_B^{\text{ref}} \quad (17)$$

where $\Delta H_f^{A_aB_b}$ and $\Delta S_f^{A_aB_b}$ are compound formation enthalpy and entropy, respectively. ${}^0G_i^{\text{ref}}$ is the Gibbs energy of the pure component (i) in its standard reference state. Four L_i in Eq. 15 are interaction parameters of two atoms between two sublattices and represent non-ideal behavior of Cu_4Ti phase. In this model only first linear interactions are included.

For performing the equilibrium calculations, it was assumed that Cu is in standard condition of FCC phase and Ti is in reference state of HCP. The optimized thermodynamics data for this system, which are listed in Table 1, were obtained from references [24–26].

In sublattice model the Gibbs energy of the phase is related to the site fractions y_i. Figure 3 shows free energy of Cu_4Ti as a function of site fractions. Site fractions vary from zero to one and composition and structure of the phases change with them. Four corner of the coordination space correspond to four different structures and concentration of Cu varies from one corner to the others as indicated by iso-concentration lines in Fig. 3b.

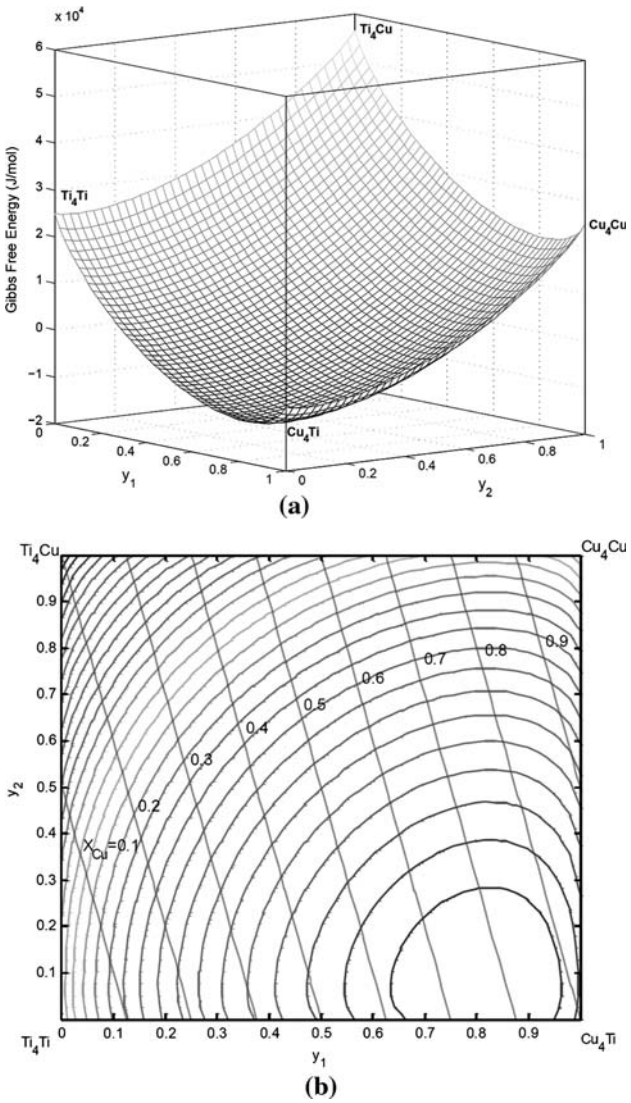

Fig. 3 (**a**) Gibbs free energy of Cu_4Ti as a function of Cu site fraction in two sublattices of $(Cu,Ti)_4(Cu,Ti)$. (**b**) Contour view of (**a**). y_1 and y_2 should be on the dotted lines in order to perform constrained minimization

Table 1 Thermodynamics properties of solution for matrix and precipitates

FCC	
$\Omega_{\text{Cu,Ti}}^0$	–9,882 J/mol
$\Omega_{\text{Cu,Ti}}^1$	115,777 J/mol
Cu_4Ti	
${}^0G_{\text{Cu:Ti}} - 4\,{}^0G_{\text{Cu}}^{\text{fcc}} - {}^0G_{\text{Ti}}^{\text{hcp}}$	5(–6011 + 2.339T)
$L_{\text{Cu,Ti:*}}$	17,089 J/mol
$L_{\text{*:Cu,Ti}}$	–15,767 J/mol

In each X_{Ti}^β, for finding $\Delta G_{\text{mix}}^\beta$ as a function of Ti molar fraction, we should optimize Eq. 15 with constrain $0.8y_{\text{Ti}}^1 + 0.2y_{\text{Ti}}^2 = X_{\text{Ti}}^\beta$. A geometrical interpretation of this procedure is choosing the minimum energy in each oblique line in Fig. 3b and connecting these points in an ordinary free energy-composition diagram. This curve is plotted in Fig. 4 for both matrix and precipitate.

After minimizing $\Delta G_{\text{mix}}^\beta$ in 500 composition points, an accurate result for unknown concentration can be obtained by a spline interpolation within these known data. For

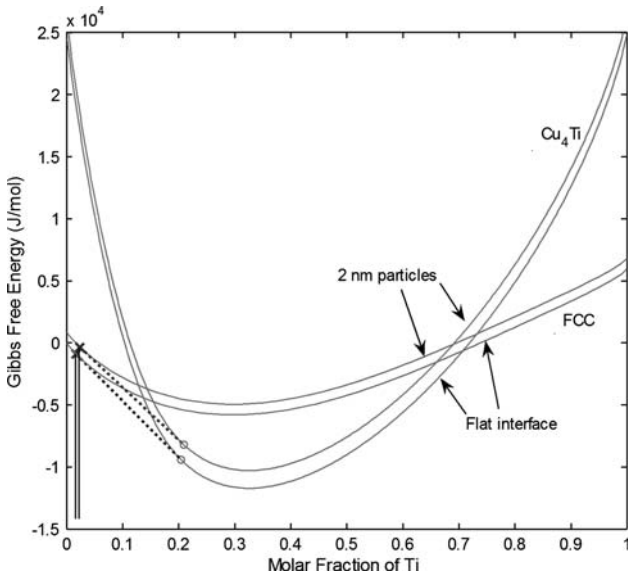

Fig. 4 Gibbs energy of matrix and precipitates in two states of bulk phase and dispersed spherical precipitates with r_p = 2 nm. Cross and circle markers show equilibrium composition of the matrix and precipitates, respectively. $\sigma_{\alpha\beta}$ was assumed to be 72 mJ/mol

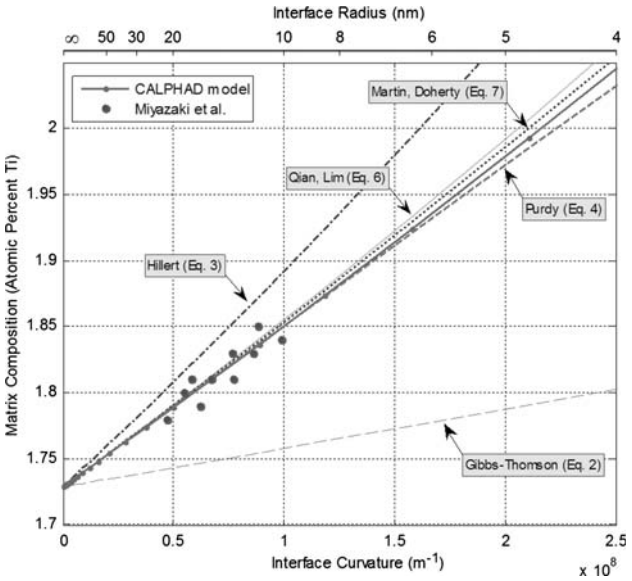

Fig. 5 Increase of matrix concentration as a function of interface radius predicted by different models with value of $\sigma_{\alpha\beta}$ = 72 mJ/mol. Interfacial energy was obtained based on best fitting of experimental data of Miyazaki et al. by CALPHAD model

$\Delta G^{\alpha}_{\text{mix}}$ we can directly use Eq. 13. Ordinary simplex or gradient base methods [27] can be used to minimize Eq. 12 and finding the equilibria.

Now, one can perform the method described in section "CALPHAD model for Gibbs–Thomson effect in binary alloys" to find the effect of interfacial curvature on increase of matrix concentration. Figure 4 shows Gibbs energy shift for matrix and precipitate with r_p = 2 nm and $\sigma_{\alpha\beta}$ = 72 mJ/mol. By assuming a value for interphase interfacial energy of the matrix and precipitates, the energy shift, ΔG_r, was calculated as a function of particle radius (Eq. 11) and was added to mixing energy of the matrix and precipitates (Eqs. 13 and 15). Total energy (Eq. 12) for an alloy X_0 = 0.1, was minimized in order to find altered equilibria in each particle radius.

The experimental data of Miyazaki et al. is plotted in Fig. 5. The unknown parameter of $\sigma_{\alpha\beta}$ in this model was changed until accurate agreement between experiments and the model was achieved. The value of $\sigma_{\alpha\beta}$ = 72 mJ/mol can fit the CALPHAD model on the experimental results. As shown in Fig. 5, with consideration of this interfacial energy, other dilute models like Hillert (Eq. 3) and Gibbs–Thomson formula (Eq. 2) are not consistent with the experiments. It should be noted that with variation of the interfacial energy, slope of the lines changes. For example if one assumes lower $\sigma_{\alpha\beta}$ (53 mJ/mol), slope of the line decreases and Hillert model fit on the data as reported by Qian and Lim [24]. Higher values of $\sigma_{\alpha\ \beta}$ fits Gibbs–Thomson formula on the data.

On the other hand, the concentrated solution models have results similar to CALPHAD model, especially at lower interfacial curvatures, where the change in concentration is small. This consistency continues in a range that the concentration variation of the matrix and precipitate is so small that the assumption of constant precipitate composition and constant Darken factor (Eq. 7) fulfills.

Conclusion

In this article, CALPHAD methodology was utilized to describe Gibbs–Thomson effect in Cu–Ti alloy which decomposes to FCC matrix and Cu_4Ti precipitates. The theory of Gibbs energy shift of the phases due to Laplace–Young pressure and interfacial energy was corrected. This new theory can truly describe energy shift of the phases and alloys which form nano-scale structures. Experimental results of Miyazaki et al. on matrix composition change versus precipitates radius were modeled By CALPHAD method. It was shown that other concentrated solution models for Gibbs–Thomson effect can also predict the concentration change. The value of 72 mJ/mol was obtained for interfacial energy of coherent Cu_4Ti precipitates. With this value, CALPHAD and other concentrated solution models give consistent results with experiments.

References

1. Lifshitz IM, Slyozov VV (1961) J Phys Chem Solids 19:35
2. Wagner C (1961) Z Elektrochem 65:581
3. Wagner R, Kampman R, Voorhees PW (2001) In: Kostorz G (ed) Phase transformations in materials. WILEY-VCH, Weinheim

4. Thomson W (Lord Kelvin) (1871) Phil Mag 42:448
5. Gibbs JW (1878) Am J Sci Ser 3:441
6. Freundlich H (1923) Colloid and capillary chemistry. Dutton, New York
7. Miyazaki T, Koyama T, Kobayashi S (1996) Metall Mater Trans A 27:945
8. Noble B, Bray SE (1999) Mater Sci Eng A 266:80
9. Hillert M (1975) In: Aaroson HI (ed) Lectures on the theory of phase transformations. TMS-AIME, New York, NY, pp 51–81
10. Purdy GR (1971) Met Sci J 5:81
11. Qian M, Lim LC (2000) Metal Mater Trans A 31:2659
12. Martin JW, Doherty RD (1976) Stability of microstructure in metallic systems. Cambridge University Press, Cambridge
13. Qian M (2002) Metal Mater Trans A 33:1283
14. Perez M (2005) Scripta Mater 52:709
15. Shirinyan A, Wautelet M, Belogorodsky Y (2006) J Phys: Condens Matter 18:2537
16. Wang CX, Yang GW (2005) Mater Sci Eng R 49:157
17. Glicksman ME (2000) Diffusion in solids: field theory, solid-state principles and application. John Wiley & Sons Inc., New York
18. Lupis CHP (1983) Chemical thermodynamic of materials. Nort-Holand: Elsevier Science, New York
19. Saunders N, Miodowink AP (1998) CALPHAD (Calculation of Phase Diagrams): a comprehensive guide. Elsevier Science Ltd
20. Kampmann R, Wagner R (1984) In: Haasen P, Gerold V, Wagner R, Ashby MF (eds) Decomposition of alloys: the early stages. Pergamon Press, New York, pp 91–103
21. Borchers C (1999) Philos Mag A 79:537
22. Borchers C, Bormann R (2005) Acta Mater 53:3695
23. Miyazaki T, Koyama T, Kobayashi S (1996) Metall Mater Trans A 27:945
24. Qian M, Lim LC (1998) Scripta Mater 39:1451
25. Kumar KCH, Ansara I, Wollants P, Delaey L (1986) Z Metallkd 87:749
26. Arroyave R, Eagar TW, Kaufman L (2003) J Alloys Comp 351:158
27. Optimization Toolbox (2005) Matlab® software documentations. Mathworks Inc